SAND2012-2569 C

SAND2012-2569C

Data-Based Stochastic Evaluation of Closed-Loop Stability and Performance

Dimitri Krattiger[1]
University of Wisconsin Madison, Madison, WI, 53715, USA

Seth L. Lacy[2] and Steven A. Lane[3]
Air Force Research Laboratory, Albuquerque, NM, 87117

Vit Babuska[4]
Sandia National Laboratories, Albuquerque, NM, 87106, USA

and

Thomas Paez[5]
MannaTech Engineering, Sandia Park, NM, 87047, USA

Metrics for determining the stability- and performance-robustness of a given controller to variations in open-loop dynamics are examined. Of particular interest are the probability distributions that these metrics have given some amount of uncertainty in the plant. The analysis herein characterizes these distributions using frequency response data collected experimentally for the open-loop plant. In doing so, it avoids using a model for the plant, thereby reducing errors and uncertainty inherent to the modeling of a plant. For a proposed controller, a Monte-Carlo method is used to evaluate the closed-loop performance and stability metrics for a large ensemble of test data and thus create an estimate of their distributions. Since ensembles of test data are typically quite small, a Karhunen-Loeve expansion based method is used to synthetically expand the set of FRFs.

Nomenclature

$\boldsymbol{x_t}$	=	Random process vector
$\boldsymbol{\mu_x}$	=	Mean vector for random process
$\boldsymbol{x_j}$	=	j^{th} experimental realization of random process vector
$\boldsymbol{V}$	=	Orthogonal basis vectors
$\boldsymbol{W}$	=	Weighting matrix
$\boldsymbol{u}$	=	Linear combination vector
$\boldsymbol{\psi}$	=	Deviation matrix
$\widehat{(\cdot)}$	=	Estimated from experimental data
n	=	Length of random process vector
q	=	Number of contributing basis vectors
M	=	Number of experimental realizations
ε	=	Smoothing parameter
$f_{\boldsymbol{u}}$	=	Kernel density estimator
$\boldsymbol{\delta}$	=	Perturbation of linear combination vector

[1] Graduate student, Department. of Engineering Physics, 1500 Engineering Drive, Rm 534.
[2] Aerospace Engineer, AFRL/RVS, 3550 Aberdeen Ave. SE, Kirtland AFB, NM 87117, AIAA Senior Member.
[3] Aerospace Engineer, AFRL/RVS, 3550 Chanute Ave. Kirtland AFB, NM, 87117, AIAA Member.
[4] Principal Member of the Technical Staff, MS 0847, PO Box 5800 Albuquerque, NM, 87185, AIAA Associate Fellow.
[5] Consultant, MannaTech Engineering, Sandia Park, NM 87047, USA, AIAA Member.

$\boldsymbol{u}_{trial}$ = Candidate combination vector
$\tilde{\boldsymbol{u}}_l^j$ = l^{th} Metropolis-Hastings Monte-Carlo generated combination vector for j^{th} test realization
P_{acc} = Probability of acceptance for candidate combination vector
r_{acc} = Acceptance parameter
$(\cdot)^{(MH)}$ = Generated using Metropolis-Hastings Monte Carlo
J_p, J_s = Performance and stability cost function
$\boldsymbol{H}, \boldsymbol{G}, \boldsymbol{Q}$ = Closed-loop, open-loop, and controller transfer functions
ω_k = k^{th} frequency point in transfer function
m = Number of outputs in transfer function
p = Number of inputs in transfer function
$\boldsymbol{M}, \boldsymbol{K}, \boldsymbol{C_D}$ = Physical Mass, Stiffness and Damping Matrices
$\boldsymbol{\mathcal{C}}_D$ = Modal damping matrix
ζ_r = Modal damping parameter for r^{th} mode
ω_r = r^{th} natural frequency
$\boldsymbol{\Phi}$ = Mode Matrix
$\boldsymbol{A}, \boldsymbol{B}, \boldsymbol{C}, \boldsymbol{D}$ = State-space matrices
$\boldsymbol{L_M}$ = Cholesky decomposition of mass matrix
$\boldsymbol{R}$ = Random matrix of zero mean, independent, normally distributed variables
$\delta_{\boldsymbol{M}}$ = Dispersion level
n_{dof} = Number of degrees of freedom in model
$n_{\boldsymbol{M}}$ = Second dimension of random matrix

I. Introduction

A major concern in control design is robustness both in stability and in performance. It is important to understand whether a nominally stable controller will become unstable or suffer in performance if the system changes or deviates from what has been modeled. Plant uncertainty can be quite significant, so it is the focus of many robustness studies including the research presented here.

Robust performance for a controller, as described in Ref. 1, is the idea that for all plants belonging to a certain set, internal stability, and performance criteria should met. Robustness calculations for single-input, single-output systems often begin with gain and phase margins for the nominal system. Large gain and phase margins are meant to ensure that small system changes don't upset the stability of the system. Ref. 2 suggests that this approach may be flawed as small parameter changes can cause the Nyquist curve to change shape resulting in large changes in gain and phase margins, and sometimes instability. Some robustness studies circumvent this issue by creating guaranteed stability bound estimates that seek to provide stability even for the worst-case plant scenario. Ref. 3 surveys several such methods and gives numerous definitions for stability including Lyapunov stability, asymptotic stability, and exponential stability. Such stability bound estimates demand that controllers are robust in stability to all possible system parameter variations and as a result are often excessively conservative and sacrifice performance. Perhaps a very small chance of instability is an acceptable tradeoff for a large improvement in performance. This notion has motivated stochastic robustness analyses, which can be used to estimate the likelihood that a system will be stable or that it will meet a defined stability criterion.

Probability of instability, as discussed by Refs. 2,4-6, uses a nominal model for the plant and introduces parameter variation through Monte Carlo simulation. It then applies a controller and analyzes the system's closed-loop eigenvalues to determine stability. A limitation of the methods described in Refs. 2,4-6, is that they require a model of the plant. Although a model is usually available, there is no guarantee that it is sufficiently accurate for closed-loop control. In fact, models invariably introduce additional uncertainty into the system due to model-form error and uncertainty in model parameter distributions. Ref. 7 proposes a method that uses test data to estimate whether or not a closed-loop system is stable. It uses a set of measurements from the plant, but doesn't require a plant model thus eliminating the difficulty of accurate identification of the plant.

The method explored in this research also relies exclusively on test data to evaluate the stability and performance of a proposed controller. Starting with a small ensemble of test data, a large synthetic ensemble is created by using a Karhunen-Loeve decomposition combined with a Kernel Density Estimator and a Metropolis-Hastings Markov Chain Monte Carlo randomization as described in Ref. 8. This expanded set of test data is then evaluated using stability and performance metrics described in Ref. 9. The derived distribution of these metrics is then used to evaluate a controller.

II. Expanding a Test Ensemble

Even for relatively simple linear plants, it is difficult to predict the changes in performance or stability in a closed-loop system resulting from parameter variation in the open-loop plant. For this reason, Monte Carlo simulation is a valuable tool. It can easily evaluate a large ensemble of perturbed systems to give a distribution of stability and performance results. This is a relatively straightforward process when a parameterized model is available for the open-loop plant. The focus of this research is to understand the performance- and stability-robustness of a proposed controller without access to a parameterized model of the open-loop plant. For this reason, the Monte Carlo simulation begins with a set of test data consisting of a frequency response function for each test realization. In order to perform the Monte Carlo simulation, additional synthetic realizations are created from an estimated probability density function of the open-loop plant.

The method used to expand the test ensemble begins with a Karhunen-Loeve expansion (KLE) as described in Ref. 8. The KLE can be used to represent a nonstationary random process. A special case of this is the representation of a univariate, continuous valued, discrete parameterized, nonstationary random process. The random process of interest is $\boldsymbol{x_t} \in \mathbb{R}^n$, and is created by stacking all of the input-output channels of the MIMO frequency response function, real and then imaginary. n is determined by the number of frequencies used in the FRF, and the number of input-output channels included. This vector random process can be described as a deviation from a mean vector $\boldsymbol{\mu_x} \in \mathbb{R}^n$, where the deviation is represented using a singular value decomposition,

$$\boldsymbol{x_t} = \boldsymbol{\mu_x} + \boldsymbol{VWu}. \tag{1}$$

In this decomposition, $\boldsymbol{W} \in \mathbb{R}^{n\times q}$ where $n \geq q$, is a diagonal matrix that contains the singular values of the deviation from the mean. The matrix $\boldsymbol{V} \in \mathbb{R}^{n\times n}$ contains orthonormal vectors, which when added in linear combinations make up the deviation. $\boldsymbol{u} \in \mathbb{R}^q$ is a random vector which determines the contribution of each basis vector to the random process vector. The components of $\boldsymbol{u}$ correspond to the q vectors in $\boldsymbol{V}$ which contribute to the deviation (some vectors in $\boldsymbol{V}$ do not contribute at all due to the small corresponding weighting value in $\boldsymbol{W}$). The set of singular values can be truncated to the set of significant singular values. This step is omitted, but can be seen in Ref. 8. Using test data denoted by $\boldsymbol{x}_j \in \mathbb{R}^q$, $j \in \{1, \dots, M\}$ where M is the number of test realizations, the components of the KLE in Eq. (1) can be estimated. The mean vector for all of the test realizations is first subtracted from each test vector and then filled into the deviation matrix $\boldsymbol{\psi} \in \mathbb{R}^{n\times M}$.

Using a singular value decomposition of $\boldsymbol{\psi}$, the estimated KLE components $\widehat{\boldsymbol{V}} \in \mathbb{R}^{n\times n}$, $\widehat{\boldsymbol{W}} \in \mathbb{R}^{n\times M}$, and $\widehat{\boldsymbol{U}} \in \mathbb{R}^{M\times M}$ can be found so that

$$\boldsymbol{\psi} = \widehat{\boldsymbol{V}}\widehat{\boldsymbol{W}}\widehat{\boldsymbol{U}}. \tag{2}$$

For every test realization $\boldsymbol{x}_j$ there is a corresponding vector $\boldsymbol{u}_j \in \mathbb{R}^M$ such that,

$$\widehat{\boldsymbol{U}} = [\boldsymbol{u_1} \cdots \boldsymbol{u_M}] \in \mathbb{R}^{M\times M}. \tag{3}$$

The next step in generating additional realizations of $\boldsymbol{x}_j$ is to create additional realizations of $\boldsymbol{u}_j$. This requires that a joint probability density function (PDF) be created for $\boldsymbol{U}$. This can be done with the kernel density estimator (KDE) given as,

$$\hat{f}_{\boldsymbol{u}}(\boldsymbol{\alpha}) = \frac{1}{M}\sum_{j=1}^{M} \frac{1}{(2\pi\varepsilon^2)^{M/2}} \exp\left[\frac{1}{2\varepsilon^2}\left\|\boldsymbol{\alpha} - \boldsymbol{u}_j\right\|^2\right]. \tag{4}$$

In this KDE, $\boldsymbol{\alpha} \in \mathbb{R}^M$ is the vector at which the PDF is being evaluated, and $\varepsilon \in \mathbb{R}^+$ is the user selected smoothing parameter that determines the sharpness of the Gaussians about the original data vectors. A large smoothing parameter ($\varepsilon \sim 1$) increases the probability that generated samples will have large deviations from the original data. A small smoothing parameter ($\varepsilon < 0.1$) can result in a *clustering* of results around the original data points. The value can be chosen so that the model distribution matches the measured distribution.

Realizations of $\boldsymbol{u}_j$ and $\boldsymbol{x}_j$ can now be created using a Metropolis-Hastings Markov-Chain Monte-Carlo technique. This method uses a starting vector and adds some random deviation to create a trial vector. The technique then evaluates the likelihood of the trial vector occurring using the KDE. The trial vector is accepted or rejected based on this likelihood compared to the likelihood of the starting vector. If the trial vector is more likely than the starting vector, it is automatically accepted. If the trial vector is less likely than the starting point, it is accepted based on the relative probability of it occurring. For example, if the trial vector is half as likely to occur as the starting vector, it has a 50% chance of being accepted. Note that no matter how unlikely a trial vector, it still has a small chance of being selected. If the trial vector is accepted, it then becomes the next starting vector, and the process is repeated. The initial starting vector can be randomly selected, or it can be chosen to be one of the original data vectors. The steps to implement this process are outlined as follows.

1) Suppose that N_{gen} (divisible by M) additional realizations are desired. Set the initial starting vector $\tilde{\boldsymbol{u}}_0^j \in \mathbb{R}^M$ equal to the experimental vector $\boldsymbol{u}_j$. From there, repeat steps a-d until $N_c = N_{gen}/M$ realizations have been created.
   a. Create a random trial vector,
   $$\boldsymbol{u}_{trial} = \tilde{\boldsymbol{u}}_l^j + \boldsymbol{\delta}, \tag{5}$$
   where $\boldsymbol{\delta}$ is a variation vector that is small enough to allow $\boldsymbol{u}_{trial} \in \mathbb{R}^M$ to remain in the vicinity of $\tilde{\boldsymbol{u}}_l^j$.
   b. Evaluate the probability of acceptance for $\boldsymbol{u}_{trial}$ as follows:
   $$P_{acc} = \frac{\hat{f}_{\boldsymbol{u}}(\boldsymbol{u}_{trial})}{\hat{f}_{\boldsymbol{u}}(\tilde{\boldsymbol{u}}_l^j)}. \tag{6}$$
   c. Find the random acceptance parameter $r_{acc} \in [0,1]$ by randomly sampling a uniform distribution from zero to one.
      i. If $P_{acc} \geq r_{acc}$, then set $\tilde{\boldsymbol{u}}_{l+1}^j = \boldsymbol{u}_{trial}$ and start again at step (a.) using $\tilde{\boldsymbol{u}}_{l+1}^j$ as the new value for $\tilde{\boldsymbol{u}}_l^j$.
      ii. If $P_{acc} < r_{acc}$ then reject $\boldsymbol{u}_{trial}$, and start again at step (a.) using the same starting vector $\tilde{\boldsymbol{u}}_l^j$ again.
2) Repeat step 1 for each of the vectors $\boldsymbol{u}_j$ in the original test ensemble.
3) Create a matrix containing all of the new realizations of $\boldsymbol{u}$,
$$\boldsymbol{U}^{(MH)} = \left\{\left[\tilde{\boldsymbol{u}}_1^1, \dots, \tilde{\boldsymbol{u}}_{N_c}^1\right], \dots, \left[\tilde{\boldsymbol{u}}_1^M, \dots, \tilde{\boldsymbol{u}}_{N_c}^M\right]\right\} \in \mathbb{R}^{M \times N_{gen}}. \tag{7}$$

With $\boldsymbol{U}^{(MH)}$ constructed, realizations of $\boldsymbol{x}_k^{(MH)} \in \mathbb{R}^n$, can be created as,
$$\boldsymbol{x}_k^{(MH)} = \boldsymbol{\mu}_{\boldsymbol{x}} + \widehat{\boldsymbol{V}}\widehat{\boldsymbol{W}}\boldsymbol{u}_k^{(MH)}, \tag{8}$$
where $k \in \{1, \dots, N_{gen}\}$, and $\boldsymbol{u}_k^{(MH)}$ is the k^{th} column of $\boldsymbol{U}^{(MH)}$.

III. Closed-Loop Evaluation

A feedback controller can be evaluated for closed-loop performance and stability. The control design approach must not be specified. In order to evaluate the closed-loop system for any particular plant realization, stability and performance cost metrics that require non-parametric open-loop system data such as frequency response are desired. Though other stability and performance metrics may also work, those in Ref. 9 are suitable for this analysis. For a system with m inputs and p outputs, defined for the frequency vector $\omega_k \in \mathbb{R}^+, k \in \{1, \dots, n_f\}$, the performance based cost function $J_p \in \mathbb{R}^+$ is defined as
$$J_p = \frac{1}{\pi}\sum_{k=1}^{n_f} tr[\boldsymbol{H}_k \boldsymbol{H}_k{}^H]\Delta\omega \tag{9}$$
$$\boldsymbol{H}_k = \boldsymbol{H}(j\omega_k) = \boldsymbol{S}(j\omega_k)\boldsymbol{G}(j\omega_k) \tag{10}$$
$$\boldsymbol{S}(j\omega_k) = [\boldsymbol{I}_{(p\times p)} + \boldsymbol{G}(j\omega_k)\boldsymbol{Q}(j\omega_k)]^{-1} \tag{11}$$
where $\boldsymbol{H} \in \mathbb{C}^{p\times m}$ is the closed-loop transfer function, $\boldsymbol{S} \in \mathbb{C}^{p\times p}$, $\boldsymbol{G} \in \mathbb{C}^{p\times m}$ is the plant realization, $\boldsymbol{Q} \in \mathbb{C}^{m\times p}$, and is the controller being implemented, and $j = \sqrt{-1}$. This control metric can be split into contributions from performance output variables, and control output variables, and weighted based on their relative importance. This process is described in Ref. 9.

The stability-based cost function $J_s \in \mathbb{R}^+$ penalizes the distance between the closed-loop transfer function and the critical point on the Nyquist plot. The stability-based cost function is defined as
$$J_s = \frac{1}{\pi}\sum_{k=1}^{n_f} \frac{1}{d^2(j\omega_k)}\Delta\omega, \tag{12}$$
where
$$d(j\omega_k) = det\left(\boldsymbol{I}_{(p\times p)} + \boldsymbol{G}(j\omega_k)\boldsymbol{Q}(j\omega_k)\right). \tag{13}$$
With the stability and performance cost metrics evaluated for each of the plant realizations, probability density function estimates can be plotted for each metric.

IV. Numerical Example

To test the method described above, a simple simulation was analyzed. It contained six masses and ten springs interconnected as shown in Fig. 1, with the nominal design values given in Table 1. Modal damping (ζ_i=3%) was

assumed. The performance output was selected to be the displacement of m_1, and the control output was selected to be the displacement of m_6. Random force inputs acted at m_4, and m_5. The nominal mass and stiffness matrices were formed for the model,

$$\boldsymbol{M} = \begin{bmatrix} m_1 & 0 & 0 & 0 & 0 & 0 \\ 0 & m_2 & 0 & 0 & 0 & 0 \\ 0 & 0 & m_3 & 0 & 0 & 0 \\ 0 & 0 & 0 & m_4 & 0 & 0 \\ 0 & 0 & 0 & 0 & m_5 & 0 \\ 0 & 0 & 0 & 0 & 0 & m_6 \end{bmatrix} \tag{14}$$

$$\boldsymbol{K} = \begin{bmatrix} k_1+k_2+k_3+k_4 & -k_2 & -k_3 & 0 & 0 & -k_4 \\ -k_2 & k_2+k_5 & 0 & 0 & 0 & -k_5 \\ -k_3 & 0 & k_3+k_6 & 0 & 0 & -k_6 \\ 0 & 0 & 0 & k_7+k_9 & 0 & -k_7 \\ 0 & 0 & 0 & 0 & k_8+k_{10} & -k_8 \\ -k_4 & -k_5 & -k_6 & -k_7 & -k_8 & k_4+k_5+k_6+k_7+k_8 \end{bmatrix}. \tag{15}$$

The modal damping matrix is given as,

$$\boldsymbol{C}_D = \begin{bmatrix} 2\zeta_1\omega_1 & 0 & 0 & 0 & 0 & 0 \\ 0 & 2\zeta_2\omega_2 & 0 & 0 & 0 & 0 \\ 0 & 0 & 2\zeta_3\omega_3 & 0 & 0 & 0 \\ 0 & 0 & 0 & 2\zeta_4\omega_4 & 0 & 0 \\ 0 & 0 & 0 & 0 & 2\zeta_5\omega_5 & 0 \\ 0 & 0 & 0 & 0 & 0 & 2\zeta_6\omega_6 \end{bmatrix} \tag{16}$$

where $\omega_r \in \mathbb{R}^+$, $r \in \{1, \dots, n_D\}$, is the r^{th} undamped natural frequency of the spring mass system, and n_D is the number of degrees of freedom (DOF) in the model. The values used in $\boldsymbol{M}$, $\boldsymbol{K}$, and $\boldsymbol{C}_D$ can be found in Table 1.

The physical damping matrix which is used in the state space model can then be computed as,

$$\boldsymbol{C_D} = \boldsymbol{M\Phi C_D \Phi^T M} \tag{17}$$

$$\boldsymbol{\Phi} = [\boldsymbol{\phi}_1, \dots \boldsymbol{\phi}_{n_D}], \tag{18}$$

where $\boldsymbol{\Phi} \in \mathbb{R}^{n_D \times n_D}$ is a matrix containing the set of mass normalized mode shapes, which solve the eigenvalue equation,

$$[\boldsymbol{K} - \omega_r{}^2 \boldsymbol{M}]\boldsymbol{\phi}_r = \boldsymbol{0}. \tag{19}$$

At this point the state-space representation containing 12 states can be formed

$$\boldsymbol{A} = \begin{bmatrix} \boldsymbol{0}_{(n_D \times n_D)} & \boldsymbol{I}_{(n_D)} \\ -\boldsymbol{M^{-1}K} & -\boldsymbol{M^{-1}C_D} \end{bmatrix} \tag{20}$$

$$\boldsymbol{B} = \begin{bmatrix} 0 \\ \boldsymbol{M^{-1}} \end{bmatrix} \tag{21}$$

$$\boldsymbol{C} = [\boldsymbol{I}_{(n_D)} \quad \boldsymbol{0}_{(n_D \times n_D)}] \tag{22}$$

$$\boldsymbol{D} = [\boldsymbol{0}]. \tag{23}$$

A positive position feedback (PPF) controller was selected to increase the damping on the 1st and 4th plant modes.

A. Synthetic Test Sample Generation

Using the maximum entropy randomization method described in Ref. 10, new realizations of the mass matrix were created,

$$\boldsymbol{M}_{rand} = \frac{1}{n_{\boldsymbol{M}}} \boldsymbol{L_M}^T (\boldsymbol{RR}^T) \boldsymbol{L_M} \tag{24}$$

$$n_{\boldsymbol{M}} = Fix\left(\frac{n_{dof}+1}{\delta_{\boldsymbol{M}}{}^2}\right), \tag{25}$$

Design Variable	Nominal Value
k_1	3000 (N/m)
k_2	1500 (N/m)
k_3	1000 (N/m)
k_4	2000 (N/m)
k_5	1100 (N/m)
k_6	1400 (N/m)
k_7	1250 (N/m)
k_8	5000 (N/m)
k_9	3000 (N/m)
k_{10}	1000 (N/m)
m_1	1.0 (kg)
m_2	1.5 (kg)
m_3	1.2 (kg)
m_4	2.0 (kg)
m_5	2.5 (kg)
m_6	1.1 (kg)
ζ_1- ζ_6	0.1 (N·s/m)

Table 1. Nominal Design Parameters. *6 DOF Spring Mass System design variables.*

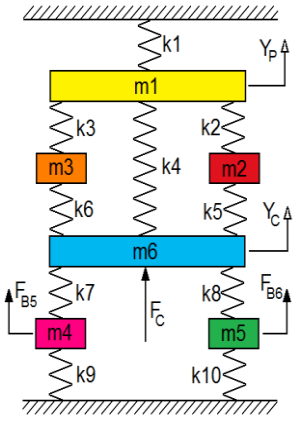

Figure 1. Six DOF Spring-mass system diagram. *Random force inputs are located at DOFs 4 and 5. A control input is located at DOF 6. Control and performance outputs are located at DOFs 6 and 1 respectively.*

where $\boldsymbol{L_M} \in \mathbb{R}^{n_{dof} \times n_{dof}}$ is the Cholesky decomposition of the nominal mass matrix, $\boldsymbol{R} \in \mathbb{R}^{n_{dof} \times n_M}$ is a matrix of independent, zero mean, unit variance, normally distributed variables, and $\delta_M \in (0,1]$ is the dispersion level, a value governing how much "randomness" is added to the nominal mass. For this example, a dispersion level of 5% was used. The operation $Fix(\cdot)$, rounds toward zero. The same process can be used for the stiffness and damping matrices to create the randomized realization of the system. Parameter variation could also have been used to create randomized systems, but doing so assumes that the model form is correct. The maximum entropy approach encompasses parameter uncertainty as well as model form uncertainty, and is thus more scalable to larger, more complex systems.

Ten realizations were created and for each of these realizations, a frequency response function was calculated. In the absence of true test data, these FRFs were treated like test data. This gives the benefit of knowing the original distribution from which the "test" samples were being drawn. Additionally, sampling this original distribution gives state-space realizations of the original distribution which can be analyzed using the methods of Refs. 2,4-6, to give a plot of the closed loop roots shown in Fig. 2. The corresponding probability of instability is zero, indicating that every realization of the original distribution is stable when paired with the controller used.

B. KLE based FRF Generation

The KLE generation method was then employed to create additional realizations of the FRF as seen in Fig. 3. As noted in Ref. 8, some of these FRFs represent physically unlikely systems. For example, some of the FRFs contain positive peaks where they should be negative and some have more than 6 peaks. Some of these systems would be considered physically unrealizable if the model form was assumed to be correct, but as mentioned above, no assumptions are made as to model form.

The smoothing parameter ε was chosen to be 0.25 using some trial-and-error iteration so that the resulting PDF estimates for the performance and stability metric didn't seem to favor the individual test values, but seemed to

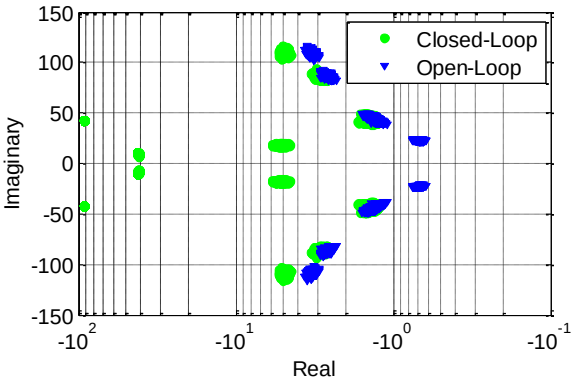

Figure 2. Root Locations for open and closed loop expected system distribution. *The loci of eigenvalues for the open-loop and closed-loop systems is shown using the set of randomly generated plants.*

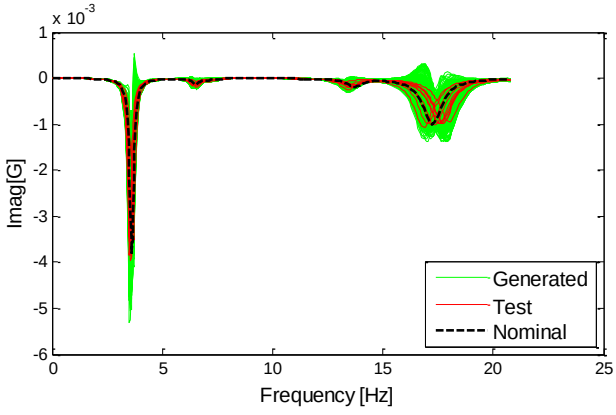

Figure 3. Imaginary component of FRF. *The imaginary component of the drive point FRF at DOF 6 is shown for the nominal system (black), the test realizations (red), and the generated systems (green).*

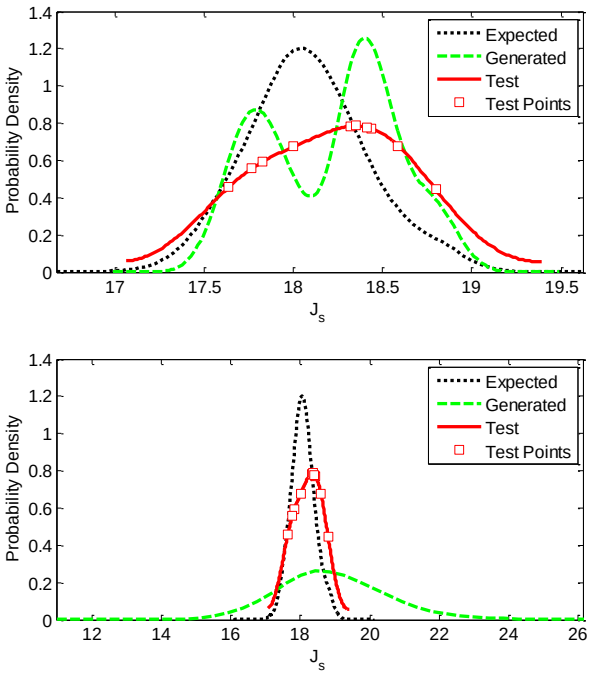

Figure 4. Examples of PDFs with badly selected smoothing parameters. *This shows probability density functions for the (closed loop) stability cost metric when plant realizations are generated with a low value of ε (top plot $\varepsilon = 0.02$), and a high value of ε (bottom plot $\varepsilon = 1.2$).*

model the whole distribution from which the test data might have come. Estimated PDFs for the stability metric are shown for values of ε that are too high, and too low in Fig. 4. Fig. 5 shows the estimated PDFs for the closed-loop performance metric for the performance output, and Fig. 6 shows the estimated PDFs for the closed-loop stability metric. Despite the unlikely FRF realizations mentioned previously, the KLE generated samples do a good job of approximating the expected distributions given the very limited amount of initial test data used.

The biggest difference between the expected and generated results is the presence of some outliers. Even when the test data is closely grouped, the KLE generation method creates a few outliers in stability metric as well as performance metric values. To investigate the cause of the outliers in stability, the plant realizations that gave the maximum and minimum values for the stability metric were analyzed. Fig. 7 shows the open-loop and closed-loop FRFs for these maximum and minimum systems. Fig. 8 shows the Nyquist plot for the closed-loop systems in Fig. 7. It is apparent from the Nyquist plot that the points leading up to the first mode are closest to the critical point and thus contribute most to the stability metric. The FRFs show that the variations in magnitude for the points leading up to the first mode are very small in the open-loop, and are only slightly larger in the closed-loop. Nevertheless, this variation accounts for the majority of the variation in the stability metric. Note that both the maximum and minimum FRFs have some KLE generated abnormalities compared to the nominal, but these have little effect on their stability metric outcomes because they are "well behaved" at low frequencies.

Similar analysis of the performance metric maximum and minimum indicates that the performance metric is more sensitive to the abnormal FRFs. The performance metric penalizes FRFs which have large magnitudes. The largest magnitudes occur at the natural frequencies, and the controller is designed to increase the damping at the modal frequencies. When open-loop plant realizations have large peaks at frequencies that are even slightly shifted from those that the controller is designed for, the result is large magnitudes in the closed-loop FRF, and large performance-metric values. The effect is that the estimated distributions are shifted right as seen in Fig. 5.

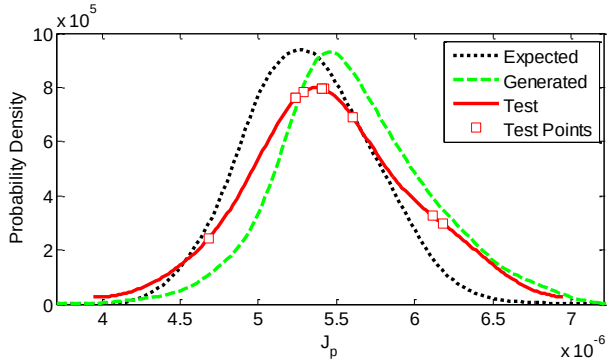

Figure 5. Estimated performance metric probability distribution function. *This plot shows the expected distribution of closed-loop performance cost (black), as well as the estimated performance cost distributions for the test realizations (red), and the generated realizations (green).*

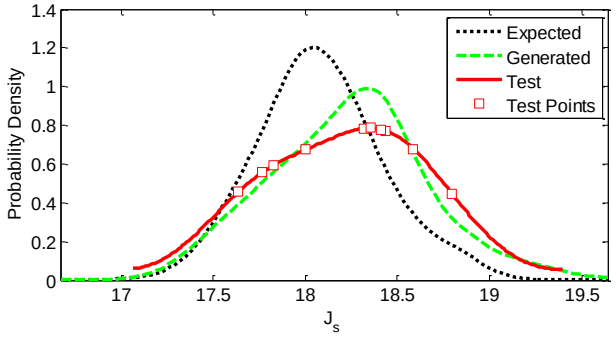

Figure 6. Estimated stability metric probability distribution function. *This plot shows the expected distribution of closed-loop stability cost (black), as well as the estimated stability cost distributions for the test realizations (red), and the generated realizations (green).*

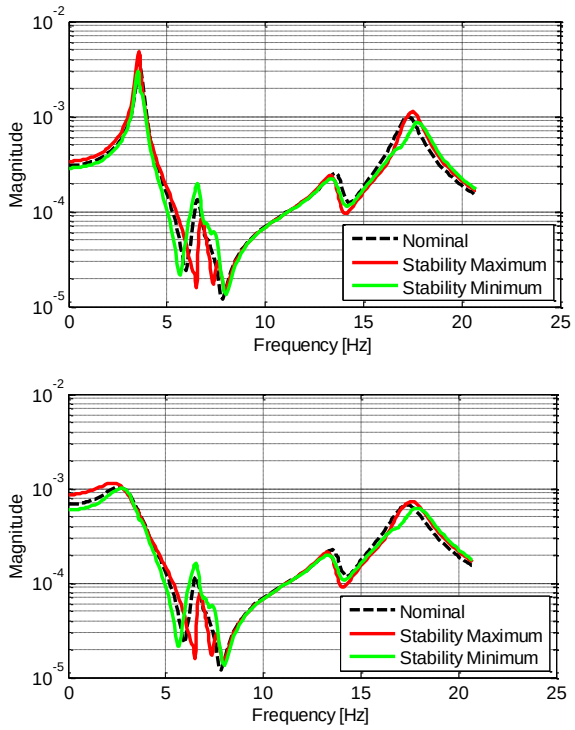

Figure 7. Open- and closed-loop stability curves. *The top plot shows the open-loop FRFs that led to the maximum (red), and minimum (green) stability cost. Also shown is the nominal FRF (black). The bottom plot shows the same thing for the closed-loop system.*

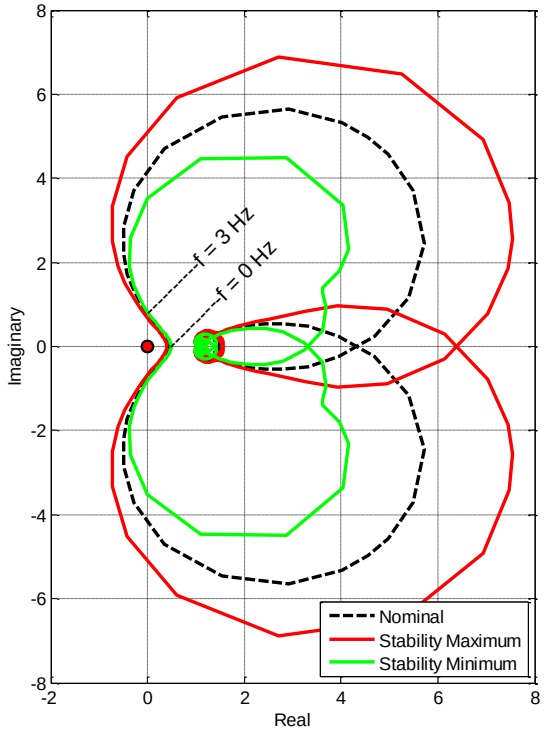

Figure 8. Nyquist Contours. *This plot shows the Nyquist contours for the closed loop systems that led to the maximum (red) and minimum (green) stability cost. Also shown is the nominal system Nyquist curve (black).*

V. Conclusion

The analysis in this paper attempts to estimate the effects of plant uncertainty on the closed-loop controller. It does so using small sets of FRF data allowing test results without models to be used in the evaluation of a controller. This reduces the amount of uncertainty in the analysis because no model uncertainty is added.

Certain problems are inherent to the use of small data sets in estimating PDFs. A single outlier, for example can skew the results quite a bit. For this reason, large outliers in the test data may warrant exclusion from the analysis. Many of the difficulties encountered with the techniques used revolve around the abnormal FRFs created by the KLE generation method. For this reason, other methods for FRF generation are being explored. Auto-Regressive-Moving-Average (ARMA) parameterization, for example does a good job creating FRFs without abnormalities, but has difficulties when the FRFs have closely spaced modes. The ARMA method also requires some prior knowledge of the original system (such as number of modes) that is not necessary with the methods used in this paper. Another approach that has shown promise includes constraints in the KLE generation method to weed out abnormal realizations.

Further work may attempt to refine the techniques used to generate the FRFs. This will involve developing more concrete guidelines to the choosing of the smoothing parameter. Further investigations could also include a wider array of controllers (perhaps some that are less sensitive to frequency shifts).

Acknowledgments

A portion of this work was performed at Sandia National Laboratories. Sandia National Laboratories is a multi-program laboratory managed and operated by Sandia Corporation, a wholly owned subsidiary of Lockheed Martin Corporation, for the U.S. Department of Energy's National Nuclear Security Administration under contract DE-AC04-94AL85000. A part of this work was supported by the Air Force Research Laboratory Space Vehicles Directorate under contract FA9453-09-C-0362 and the Air Force Office of Scientific Research. Mr. Krattiger contributed to this research under the AFRL Space Scholar Program in 2011.

References

[1]J. C. Doyle, B. A. Francis, A. R. Tannenbaum, *Feedback Control Theory*, Macmillan, New York, 1992, pp 46-61.

[2]R. F. Stengel, L. R. Ray, And C. I. Marrison, "Probabilistic Evaluation of Control System Robustness," *International Journal of Systems*, 1995.

[3]F. Kozin, "A Survey of Stability of Stochastic Systems", *Automatica*, vol. 5, pp. 95-112, 1969.

[4]L. R. Ray And R. F. Stengel , "A Monte Carlo Approach to the Analysis of Control System Robustness," *Automatica*, vol 29, No. 1, pp. 229-236, 1993.

[5]R. F. Stengel And L. R. Ray, "Stochastic Robustness of Linear Time-Invariant Control Systems," *IEEE Transactions on Automatic Control*, vol 36, No. 1, pp. 82-87, 1991.

[6]R. F. Stengel, "Some Effects of Parameter Variations on the Lateral-Directional Stability of Aircraft," *J. Guidance and Control*, vol 3, No. 2, pp. 124-131, 1980.

[7]K. V'Heusden, A. Karimi And D. Bonvin, "Data Driven Controller Validation," Presented at the 15th IFAC Symposium on System Identification, 2009.

[8]T. L. Paez, S. L. Lacy, And V. Babuska, "Improved Stochastic Process Models for Linear Structure Behavior," *Proceedings of the American Control Conference*, pp. 1139-1144, 2009.

[9]M. Holzel, S. L. Lacy, V. Babuska, And D. Bernstein, "Direct Frequency Response Based, Uncertainty Accomodating Optimal Control Design," Presented at the American Control Conference, 2009.

[10]C. Soize, "Maximum Entropy Approach for Modeling Random Uncertainties in Transient Elastodynamics," *Journal of the Acoustical Society of America*, vol. 109 (5), Pt. 1, 2001.